Diyala Journal of Engineering Sciences, Vol. 11, No. 2, June 2018, pages 55-59 ISSN 1999-8716
DOI: 10.24237/djes.2018.11207 eISSN 2616-6909

Theoretical Analysis of Fiber Bragg Grating Tunable Filter Utilizing Tensile /Compression Technique

Ayad Z. Mohammed, A. K. Abass *, Samar K. Ibrahim Wail Yass Nassir
Department of Laser and Optoelectronics Engineering, University of Technology, Iraq
140042@uotechnology.edu.iq

Abstract

In this paper a wideband tunable filter based on fiber Bragg grating (TF-FBG) utilizing tensile/ compression technique is theoretically investigated. According to the results, a wide tuning range is achieved about 48.36 nm in C-band region from 1513.7 nm to 1562.1 nm; 12.09 nm for tension and 36.27 nm for compression (C-band refers to the wavelength range 1530–1565 nm). While, for L-band region the wavelength shift is slightly greater than in the C-band region about 49.272 nm from 1543 nm to 1592.3 nm; 12.3 nm for tension and 36.972 nm for compression (L-band refers to the wavelength range 1565 – 1625 nm).

Keywords: Fiber Bragg grating; tunable filter; tensile/compression technique.
Paper History: Received: (4/10/2016), Accepted: (29/12/2016)

Introduction

Fiber Bragg gratings (FBGs) have been investigated in many published works during recent decades and up to the present. This is due to their applications as attractive optical sensors for different measurement purposes [1-4]. At the same time tunable optical filters based on FBGs are widely used for semiconductor and doped fiber lasers [5-7], gain equalizer in a fiber amplifier [8], as well as add/drop multiplexer for wavelength division multiplexing systems [9].
In this context, the FBG center wavelength can be tuned by adjusting the refractive index of the fiber or by modifying the grating period. These modifications can be achieved by different ways, such as thermal effects [10-12], electromagnetic force [13], mechanical effect [14, 15] and pressure technique [16]. Typically, the required FBG tuning range is up to 45 nm in order to cover the whole gain bandwidth of the EDFA or Raman fiber amplifier. This tuning range cannot be carried out either by heating or by pressure techniques. While up to 50 nm was achieved utilizing the mechanical technique within faster response [17].
In this paper, a FBG-TF via tensile/compression technique is theoretically analysis. Two optical bands are investigated, namely, C-band and L-band in order to cover the gain bandwidth of the hybrid EDFA/ Raman fiber amplifier. In C-band region, up to 48.36 nm shift in the center wavelength is achieved; 12.09 nm in tension and 36.27 nm for compression. While, for L-band region the wavelength shift is slightly greater than in the C-band region about 49.272 nm is obtained; 12.3 nm in tension and 36.972 nm for compression.

Theoretical Model:

A fiber Bragg grating is a piece of optical fiber with a periodic variation of the index of refraction along the fiber axis. Such a phase grating acts as a band rejection filter reflecting wavelengths that satisfy the Bragg condition and transmitting the others. FBGs act like tiny mirrors in a fiber that reflect specific wavelengths due to periodic changes in the index of the fiber core.
In a uniform FBG, the length period of refractive index change Λ is fixed and usually Λ is around 0.5 μm.
Coherent reflection is achieved where the period is half the wavelength of the light in the fiber, giving an equation known as the Bragg condition:

$$\boldsymbol{N}\,.\,\boldsymbol{\lambda_B} = \mathbf{2}\,\boldsymbol{n_{eff}}\,\boldsymbol{\Lambda_g} \qquad (1)$$

where N ≥ 1 is an integer indicating the order of the grating period, $\boldsymbol{\lambda_B}$ is Bragg wavelength, $\boldsymbol{\Lambda_g}$ is grating period, $\mathbf{n_{eff}}$ is the Effective refractive index of the transmitting medium.
Using the coupled-mode theory, theoretically the normalized reflection produced by an FBG is given by:

$$\boldsymbol{R} = |\boldsymbol{\rho}|^{\mathbf{2}} = \frac{\boldsymbol{sinh^2(\varphi L)}}{\boldsymbol{cosh^2(\varphi L)} - \frac{\boldsymbol{\delta^2}}{\boldsymbol{k^2}}} \qquad (2)$$

where $\boldsymbol{\rho}$ is the reflection coefficient of the grating, **L** is the grating length, **δ** is the detuning parameter and it is:

$$\boldsymbol{\delta} = \frac{2\pi n_{eff}}{\lambda} - \frac{\pi}{\Lambda} \quad (3)$$

$$\boldsymbol{\varphi} = \sqrt{\boldsymbol{k^2 - \delta^2}} \quad (4)$$

κ is the coupling coefficient, $\boldsymbol{\kappa} = \frac{\pi \Delta n}{\lambda} \boldsymbol{\eta}$

$\boldsymbol{\eta}$ is the overlap integral and can be approximated as η ≈1 for single mode fibers with step index. In this case, $\boldsymbol{\eta = \Delta n\, F}$, **F** is the fractional modal power in the core given by:

$$\mathbf{F} = \left[\mathbf{1} - {}^{\mathbf{1}}/_{\mathbf{V}^2}\right] \quad (5)$$

where **V** is the normalized frequency and **Δn** is the amplitude of induced refractive index perturbation.
The shift in Bragg wavelength with applied strain is described as the following Equation [17]:

$$\frac{\Delta\lambda}{\lambda_{Bo}} = (\mathbf{1} - \mathbf{p_e})\, \boldsymbol{\varepsilon_{ax}} \quad (6)$$

where **Δλ** is the wavelength shift, $\boldsymbol{\lambda_{Bo}}$ is Bragg wavelength, $\boldsymbol{p_e}$ is the effective photoelastic constant it is about 0.22, $\boldsymbol{\varepsilon_{ax}}$ is the axial strain (tensile or compressive) applied on the FBG.
Equation 6 can be re-write as following and the new Bragg wavelength (λ_B) become:

$$\boldsymbol{\lambda_B = \lambda_{Bo} \pm \lambda_{Bo}(0.78 * \varepsilon_{ax})} \quad (7)$$

The minus sign should be used in the compression technique.

Table 1 Simulation parameters.

Bragg wavelength, λ_B	1550 nm for C-band 1580 nm for L-band
Radius of core, a	4.1μm
Effective refractive index, n_{eff}	1.444 when λ= 1550 nm 1.4437 when λ= 1580 nm
Grating length, L	15 mm
Index difference between core and cladding, Δn	0.0036
Axial strain, ε_{ax}	0 to 0.01 steps of 0.002 for tensile, and 0 to 0.03 steps of 0.003 for compression

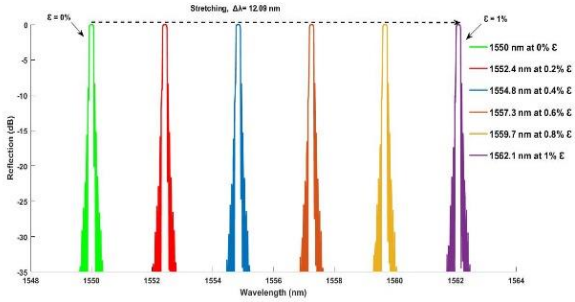

Figure 1: Reflection spectra of a 15 mm FBG with center wavelength 1550 nm via stretching technique

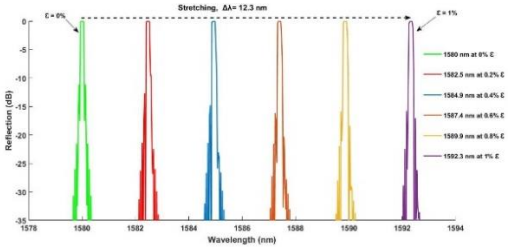

Figure 2: Reflection spectra of a 15 mm FBG with center wavelength 1580 nm via stretching technique

For the compression method, Figure 3 and 4 show the reflection spectra for a proposed optical filter in the C-band region (1550 nm) and L-band region (1580 nm), respectively. The increasing in compressive strain $\boldsymbol{\varepsilon_{ax}}$ from 0 % to 3% showed blue shifting in the center wavelength about 36.27 nm at C-band and 36.972 nm at L-band. Typically, an optical fiber is up to 20 times stronger in compression than that in tension according to the mechanical properties of FBG [17]. When a compressive axial strain is applied to the unstrained FBG, theoretically the same wavelength shift of axial strain will be achieved but, in this case, the grating period will decrease which will cause the reflectivity peak to shift towards the left side to a new Bragg wavelength value (blue shift); i.e., a negative wavelength shift will be achieved.

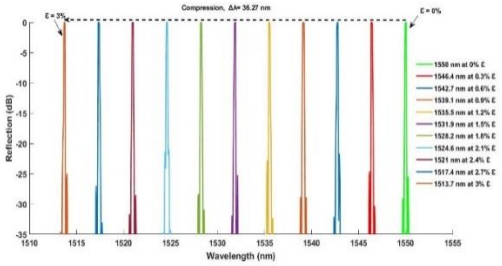

Figure 3: Reflection spectra of a 15mm FBG with center wavelength 1550 nm via compression technique

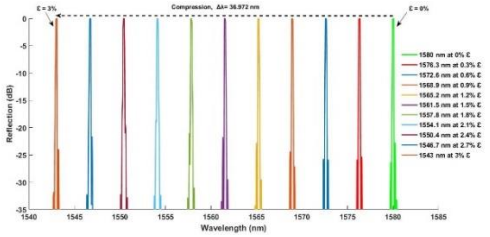

Figure 4: Reflection spectra of a 15mm FBG with center wavelength 1580 nm via compression technique

1> Appendix A: Theoretical analysis flowchart

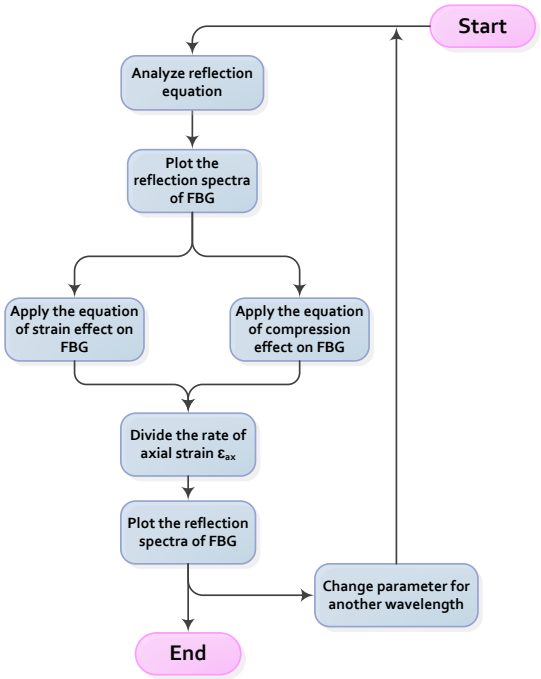

Figure 5: Flowchart of processes for theoretical analysis

2> Appendix B: MATLAB code for stretching

```
clc
clear all
del=0.0036; %index difference between core and clad
neff=1.444;      %effective refractive for mode
lamo=1550*10.^-9          %centre wavelength
a=4.1*10.^-6;                %radious of core
cap=lamo/(2*neff);        %pitch of the grating
deln=1.8*10.^-4;  %index amplitude of grating
lam=linspace(1549*10.^-9,1565*10.^-9,1000);%wavelengths of the source
l=15*10.^-3;                  %grating length
for i=1:1000
beta=2*pi*neff/lam(i);              %propogation constant of the mode
delta=beta-(pi/cap);              %detuning vector
v=2*pi*a*neff*sqrt(2*del)/lam(i); %v-number
f=(1-1/v.^2);     %fraction of the integrated fundamental-mode intensity contained in the core
eta=deln*f;
k=pi*eta/lam(i);            %coupling coefficient
r1=sinh(sqrt(k.^2-delta.^2)*l)*sinh(sqrt(k.^2-delta.^2)*l);
r2=cosh(sqrt(k.^2-delta.^2)*l)*cosh(sqrt(k.^2-delta.^2)*l);
r3=(delta/k)*(delta/k);
R1(i)=10*log(r1/(r2-r3));          %reflectivity of grating
end
del=0.0036;          %index difference between core and clad
neff=1.444;      %effective refractive for mode
lamo=1550*10.^-9;          %centre wavelength
lamb1=(0.78*lamo*0.002)+lamo
a=4.1*10.^-6;                %radious of core
cap=lamb1/(2*neff);        %pitch of the grating
deln=1.8*10.^-4;  %index amplitude of grating
lam=linspace(1549*10.^-9,1565*10.^-9,1000);%wavelengths of the source
l=15*10.^-3;                  %grating length
for i=1:1000
beta=2*pi*neff/lam(i);              %propogation constant of the mode
delta=beta-(pi/cap);              %detuning vector
v=2*pi*a*neff*sqrt(2*del)/lam(i); %v-number
f=(1-1/v.^2);     %fraction of the integrated fundamental-mode intensity contained in the core
eta=deln*f;
k=pi*eta/lam(i);            %coupling coefficient
r1=sinh(sqrt(k.^2-delta.^2)*l)*sinh(sqrt(k.^2-delta.^2)*l);
r2=cosh(sqrt(k.^2-delta.^2)*l)*cosh(sqrt(k.^2-delta.^2)*l);
r3=(delta/k)*(delta/k);
R2(i)=10*log(r1/(r2-r3));     %reflectivity of grating
```

```
end
del=0.0036;
neff=1.444;
lamo=1550*10.^-9;
lamb2=(0.78*lamo*0.004)+lamo
a=4.1*10.^-6;
cap=lamb2/(2*neff);
deln=1.8*10.^-4;
lam=linspace(1549*10.^-9,1565*10.^-9,1000);
l=15*10.^-3;
for i=1:1000
beta=2*pi*neff/lam(i);
delta=beta-(pi/cap);
v=2*pi*a*neff*sqrt(2*del)/lam(i);
f=(1-1/v.^2);
eta=deln*f;
k=pi*eta/lam(i);
r1=sinh(sqrt(k.^2-delta.^2)*l)*sinh(sqrt(k.^2-
delta.^2)*l);
r2=cosh(sqrt(k.^2-delta.^2)*l)*cosh(sqrt(k.^2-
delta.^2)*l);
r3=(delta/k)*(delta/k);
R3(i)=10*log(r1/(r2-r3));
end
del=0.0036;
neff=1.444;
lamo=1550*10.^-9;
lamb3=(0.78*lamo*0.006)+lamo
a=4.1*10.^-6;
cap=lamb3/(2*neff);
deln=1.8*10.^-4;
lam=linspace(1549*10.^-9,1565*10.^-9,1000);
l=15*10.^-3;
for i=1:1000
beta=2*pi*neff/lam(i);
delta=beta-(pi/cap);
v=2*pi*a*neff*sqrt(2*del)/lam(i);
f=(1-1/v.^2);
eta=deln*f;
k=pi*eta/lam(i);
r1=sinh(sqrt(k.^2-delta.^2)*l)*sinh(sqrt(k.^2-
delta.^2)*l);
r2=cosh(sqrt(k.^2-delta.^2)*l)*cosh(sqrt(k.^2-
delta.^2)*l);
r3=(delta/k)*(delta/k);
R4(i)=10*log(r1/(r2-r3));
end
del=0.0036;
neff=1.444;
lamo=1550*10.^-9;
lamb4=(0.78*lamo*0.008)+lamo
a=4.1*10.^-6;
cap=lamb4/(2*neff);
deln=1.8*10.^-4;
lam=linspace(1549*10.^-9,1565*10.^-9,1000);
l=15*10.^-3;
for i=1:1000
beta=2*pi*neff/lam(i);
delta=beta-(pi/cap);
v=2*pi*a*neff*sqrt(2*del)/lam(i);
f=(1-1/v.^2);
eta=deln*f;
k=pi*eta/lam(i);
r1=sinh(sqrt(k.^2-delta.^2)*l)*sinh(sqrt(k.^2-
delta.^2)*l);
r2=cosh(sqrt(k.^2-delta.^2)*l)*cosh(sqrt(k.^2-
delta.^2)*l);
r3=(delta/k)*(delta/k);
R5(i)=10*log(r1/(r2-r3));
end
del=0.0036;
neff=1.444;
lamo=1550*10.^-9;
lamb5=(0.78*lamo*0.01)+lamo
a=4.1*10.^-6;
cap=lamb5/(2*neff);
deln=1.8*10.^-4;
lam=linspace(1549*10.^-9,1565*10.^-9,1000);
l=15*10.^-3;
for i=1:1000
beta=2*pi*neff/lam(i);
delta=beta-(pi/cap);
v=2*pi*a*neff*sqrt(2*del)/lam(i);
f=(1-1/v.^2);
eta=deln*f;
k=pi*eta/lam(i);
r1=sinh(sqrt(k.^2-delta.^2)*l)*sinh(sqrt(k.^2-
delta.^2)*l);
r2=cosh(sqrt(k.^2-delta.^2)*l)*cosh(sqrt(k.^2-
delta.^2)*l);
r3=(delta/k)*(delta/k);
R6(i)=10*log(r1/(r2-r3));
end
plot(lam,R1,'g',lam,R2,'r',lam,R3,lam,R4,lam,
R5,lam,R6)
ylim([-35 0])
```

References

[1] J. H. Ng, X. Zhou, X. Yang, and J. Hao, A simple temperature-insensitive fiber Bragg grating displacement sensor, Opt. Commun., 273, (2), (2007), 398–401.

[2] J. A. S. Dias, R. L. Leite, and E. C. Ferreira, Electronic technique for temperature compensation of fibre Bragg gratings sensors, Int. J. Electron. Commun., 62, (1), (2008), 72–76.

[3] M. Rosenberger, S. Hessler, S. Belle, B. Schmauss, and R. Hellmann, Compressive and tensile strain sensing using a polymer planar Bragg grating, Opt. Soc. Am., 22, (5), (2014), 5483–5490.

[4] Z. Yu, Q. Jiang, H. Zhang, and J. Wang, Theoretical and experimental investigation of fiber Bragg gratings with different lengths for ultrasonic detection, Springerlink, 6, (2), (2016), 187–192.

[5] R. A. Drainville and G. Das, Widely Tunable Fiber Bragg Grating and its Application in Fiber Lasers, Microw. Opt. Technol. Lett., 55, (12), (2013), 2824–2826.

[6] L. Wang, J. Ren, H. Li, T. Zhao, Q. Xu, X. Changa, and L. Zhao, Fiber Bragg grating and its application in external cavity semiconductor laser, Opt. - Int. J. Light Electron Opt., 124, (19), (2013), 3816–3818.

[7] S. Liaw, K. Hung, Y. Lin, C.-C. Chiang, and C.-S. Shin, C-band continuously tunable lasers using tunable fiber Bragg gratings, Opt. Laser Technol., 39, (6), (2007), 1214–1217.

[8] M. Tang, Y. D. Gong, and P. Shum, Dynamic Properties of Double-Pass Discrete Raman Amplifier With FBG-Based All-Optical Gain Clamping Techniques, IEEE Photonics Technol. Lett., 16, (3), (2004), 768–770.

[9] A. Iocco, H. G. Limberger, R. P. S. E, L. A. Everall, K. E. Chisholm, J. A. R. Williams, and I. Bennion, Bragg grating fast tunable filter for wavelength division multiplexing, J. Light. Technol., 17, (7), (1999), 1217–1221.

[10] S. Y. Li, N. Q. Ngo, S. C. Tjin, P. Shum, and J. Zhang, Thermally tunable narrow-bandpass filter based on a linearly chirped fiber Bragg grating, Opt. Lett., 29, (1), (2004), 29–31.

[11] L. Huang, P. Ma, R. Tao, C. Shi, X. Wang, and P. Zhou, Experimental investigation of thermal effects and PCT on FBGs-based linearly polarized fiber laser performance, Opt. Soc. Am., 23, (8), (2015), 10506–10520.

[12] B. A. Ribeiro, M. M. Werneck, F. B. V. de Nazaré, and M. N. Gonçalves, A Bragg grating tunable filter based on temperature control system to demodulate a voltage sensor, in International Conference on Optical Fibre Sensors, 2015.

[13] H. A. Fayed, M. Mahmoud, A. K. Aboulseoud, and M. H. Aly, "A Wide Range Tunable Fiber Bragg Grating Using Fast Changeable Electromagnetic Force," in *Photonics North*, 7750, (77501R–1–10), (2010).

[14] N. Mohammad, W. Szyszkowski, W. J. Zhang, E. I. Haddad, J. Zou, W. Jamroz, and R. Kruzelecky, "Analysis and development of a tunable fiber Bragg grating filter based on axial tension/compression," *J. Light. Technol.*, 22, (8), (2004), 2001–2013.

[15] A. A. S. Falah, M. R. Mokhtar, Z. Yusoff, and M. Ibsen, Reconfigurable Phase-Shifted Fiber Bragg Grating Using Localized Micro-Strain, IEEE Photonics Technol. Lett., 28, (9), (2016), 951–954.

[16] G. Chen, L. Liu, H. Jia, J. Yu, L. Xu, and W. Wang, Simultaneous pressure and temperature measurement using Hi-Bi fiber Bragg gratings, *Opt. Commun.*, 228, (1–3), (2003), 99–105.

[17] N. Mohammad, Analysis and Development of a Tunable Fiber Bragg Grating Filter Based on Axial Tension / Compression, 2005.